Ultrasound in Med. & Biol., Vol. ■, No. ■, pp. 1–8, 2012

0301-5629/$ - see front matter

http://dx.doi.org/10.1016/j.ultrasmedbio.2012.09.024

● *Original Contribution*

# CLINICAL ASSESSMENT OF THE 1/3 RADIUS USING A NEW DESKTOP ULTRASONIC BONE DENSITOMETER

EMILY M. STEIN,* FERNANDO ROSETE,* POLLY YOUNG,* MAFO KAMANDA-KOSSEH,* DONALD J. MCMAHON,* GANGMING LUO,†‡ JONATHAN J. KAUFMAN,†§ ELIZABETH SHANE,* and ROBERT S. SIFFERT§

*Department of Medicine, Columbia University College of Physicians and Surgeons, New York, NY, USA; †CyberLogic, Inc., New York, NY, USA; ‡Department of Rehabilitation Medicine, New York University School of Medicine, New York, NY, USA; and §Department of Orthopedics, The Mount Sinai School of Medicine, New York, NY, USA

(*Received* 28 *March* 2012; *revised* 20 *September* 2012; *in final form* 27 *September* 2012)

**Abstract—The objectives of this study were to evaluate the capability of a novel ultrasound device to clinically estimate bone mineral density (BMD) at the 1/3 radius. The device rests on a desktop and is portable, and permits real-time evaluation of the radial BMD. The device measures two net time delay (NTD) parameters, $NTD_{DW}$ and $NTD_{CW}$. $NTD_{DW}$ is defined as the difference between the transit time of an ultrasound pulse to travel through soft-tissue, cortex and medullary cavity, and the transit time through soft tissue only of equal overall distance. $NTD_{CW}$ is defined as the difference between the transit time of an ultrasound pulse to travel through soft-tissue and cortex only, and the transit time through soft tissue only again of equal overall distance. The square root of the product of these two parameters is a measure of the radial BMD at the 1/3 location as measured by dual-energy X-ray absorptiometry (DXA). A clinical IRB-approved study measured ultrasonically 60 adults at the 1/3 radius. BMD was also measured at the same anatomic site and time using DXA. A linear regression using NTD produced a linear correlation coefficient of 0.93 ($p < 0.001$). These results are consistent with previously reported simulation and *in vitro* studies. In conclusion, although X-ray methods are effective in bone mass assessment, osteoporosis remains one of the largest undiagnosed and under-diagnosed diseases in the world today. The research described here should enable significant expansion of diagnosis and monitoring of osteoporosis through a desktop device that ultrasonically assesses bone mass at the 1/3 radius. (E-mail: jjkaufman@cyberlogic.org)** © **2012 World Federation for Ultrasound in Medicine & Biology.**

*Key Words:* **Osteoporosis, Bone mineral density, Ultrasound, Net time delay, DXA, Radius.**

## INTRODUCTION

The objective of this study is to enhance the ability of ultrasound to noninvasively assess bone. As is well known, osteoporotic fractures are a major public health problem associated with high degrees of morbidity and mortality (Miller 1978; Melton 1988; Anonymous 2001; Kanis 2002; Kanis et al. 2009a). As stated on the National Osteoporosis Foundation (NOF) website <nof.org>, osteoporosis and low bone mass are currently estimated to be a major public health threat for almost 44 million US women and men aged 50 and older. The 44 million people with either osteoporosis or low bone mass represent 55% of the people aged 50 and older in the United States. According to estimated figures, osteoporosis was responsible for more than 2 million fractures in 2005, including approximately 297,000 hip fractures, 547,000 vertebral fractures, 397,000 wrist fractures, 135,000 pelvic fractures and 675,000 fractures at other sites. The number of fractures attributable to osteoporosis is expected to rise to more than 3 million by 2025. If current trends continue, the number of people affected with osteoporosis or osteopenia will climb to over 61 million by 2020. In 2005, osteoporosis-related fractures were responsible for an estimated $19 billion in costs, and by 2025, it is predicted that these costs will rise to approximately $25.3 billion. The toll both in individual quality of life and in national health care costs of osteoporotic

Address correspondence to: Jonathan J. Kaufman, Ph.D., CyberLogic, Inc., 611 Broadway, Suite 707, New York, NY 10012. E-mail: jjkaufman@cyberlogic.org

Conflict of Interest: One of the authors (Jonathan J. Kaufman) is a principal and CEO of the company (CyberLogic, Inc.), which manufactures the UltraScan 650 device, and another of the authors (Gangming Luo) is an employee of the same company. None of the other authors report any conflicts of interest.

fractures cannot be overstated. Early detection and assessment is crucial to initiating therapeutic interventions as this is the best way to prevent a fracture from occurring (Kanis et al. 2009b).

Presently the gold standard for bone assessment is based on X-ray densitometric techniques, such as with dual-energy X-ray absorptiometry (DXA) (Ott et al. 1987; Kaufman and Siffert 2001; Blake and Fogelman 2003; Bonnick 2004; Johnell et al. 2005). The measurement of bone mass as represented for example by (areal) bone mineral density (BMD) is based on the well established principle that more mass is generally associated with a stronger bone, and a stronger bone is in turn associated with a reduced risk of fracture (Turner 2006). Indeed, BMD is the single most important factor in estimating bone strength and fracture risk (Baim and Leslie 2012). Notwithstanding these facts, osteoporosis remains one of the world's most under-diagnosed diseases. Indeed, the NOF estimates that only about 20% of the at-risk population has been assessed; indeed the problem of under-diagnosing osteoporosis appears to be getting worse (Lewiecki et al. 2012; Zhang et al. 2012). The reasons for this are several. First and foremost is perhaps that the vast majority of primary care physicians do not have bone assessment capability available; therefore, patients must be referred off-site to specialists for these measurements making them performed less often than necessary. In addition, the relatively high cost of such bone density tests—not always covered by health insurance—and the high costs of the devices themselves—also leads to them being utilized less frequently as needed (King and Fiorentino 2011). There is also the issue of ionizing radiation, which at least in the minds of some patients, is another reason to avoid the test (Leffall and Kripke 2010).

Ultrasound has been proposed as an alternative to DXA (Langton et al. 1984; Laugier 2008; Krieg et al. 2008). It is nonionizing, relatively (to DXA) inexpensive and as a mechanical wave may provide information above and beyond mass alone (Kaufman and Einhorn 1993; Siffert et al. 1996; Njeh et al. 2001; Siffert and Kaufman 2007; Langton and Njeh 2008; Padilla et al. 2008; Hosokawa 2010; Souzanchi et al. 2012). A number of research and/or commercial ultrasonic devices are currently available and operate in one of three basic modalities (Laugier and Haiat 2011); these include through transmission methods (Langton et al. 1984; Kaufman and Einhorn 1993; Wear 2000), pulse-echo (backscattering methods) (Wear 2008; Karjalainen et al. 2009; Litniewski et al. 2012), and axial transmission methods (Barkmann et al. 2000; Lefebvre et al. 2002; Talmant et al. 2009; Moilanen 2008; Kilappa et al. 2011). Notwithstanding the number of devices and modalities already explored, the impact that ultrasound has had to date on improving bone health and identifying those individuals at increased risk of fracture has been relatively modest. This is due primarily to the fact that performance of present ultrasound technology—and specifically performance in terms of serving as a proxy for BMD—is less than needed to displace the current gold standard, DXA. For example, presently approved thru-transmission ultrasound devices designed to measure the calcaneus provide correlations with BMD at the same anatomical site ranging from 0.6 to about 0.8 (Langton and Langton 2000). Axial and backscattering ultrasound methods produce even poorer correlations with BMD (Laugier and Haiat 2011).

The purpose of this article is to report on the ability of a new desktop ultrasound device to clinically estimate BMD at the 1/3 radius. The rest of this article is organized as follows. The next section describes the ultrasound measurement methodology, including the signal processing algorithm and the clinical study protocol. The results are then provided, followed by a discussion and conclusion that summarizes the findings of this study.

## MATERIALS AND METHODS

### *Device and signal processing*

A new desktop device (*UltraScan 650*, CyberLogic, Inc., New York, NY, USA, Fig. 1) for quantitative real-time bone assessment has been constructed (Kaufman et al. 2009a). It processes ultrasound signals after propagating through a forearm and displays an estimate of BMD on a laptop computer that is connected *via* USB. The device is constructed around a 1 × 4.8 cm rectangular single element source transducer and a 1 × 4.8 cm 64 element array receiver transducer with a pitch of 0.75 mm and both transducers are flat (unfocussed). The device emits a 3.5 MHz broadband ultrasound signal from the source that propagates through the radius and

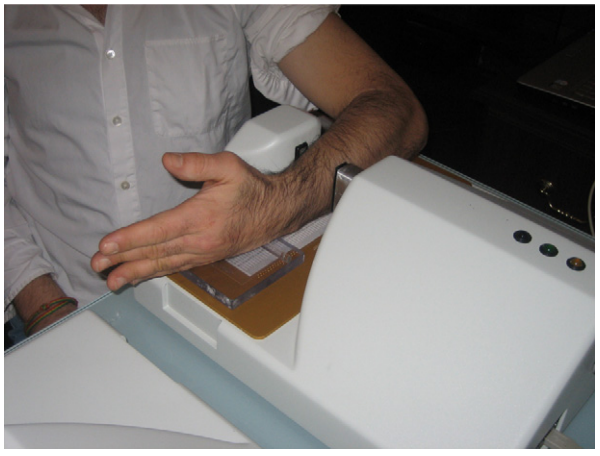

Fig. 1. The *UltraScan 650* ultrasound bone assessment device.

soft tissue to the array receiver. In water, the received waveform has a nominal center frequency of 3 MHz with a 3 dB bandwidth of 800 kHz.

In operation, the source emits a broadband ultrasonic pulse at a rate of 1 kHz, the receiver waveforms are sampled at a 50 MHz sampling rate and for each channel 64 of the received sampled-waveforms are summed to obtain an averaged set of 64 received waveforms. A variable gain under software control (0–40 dB in 5 dB increments) is set independently for each channel to bring the maximum absolute value of each channel as close as possible to the maximum value allowed (without saturation) as input to the analog-to-digital converter (±5 volt). Note that channels associated with propagation of ultrasound through bone required 30–40 dB of gain compared with propagation of ultrasound solely through soft tissue, which required 0 dB of gain. The averaged waveforms are then processed to obtain two ultrasound net time delay (NTD) parameters, $NTD_{DW}$ and $NTD_{CW}$, Figure 2 (Kaufman et al. 2007, 2008, 2009b; Le Floch et al. 2008a; Siffert and Kaufman 2007). $NTD_{DW}$, the DW notating "direct wave", is defined as the difference between the transit time of an ultrasound pulse through soft-tissue, cortex and medullary cavity, and the transit time through soft tissue only of equal overall distance. $NTD_{CW}$, the CW denoting "circumferential wave," is defined as the difference between the transit time of an ultrasound pulse through soft-tissue and cortex only and the transit time through soft tissue only again of equal overall distance. Measurement of the two NTDs and associated BMD estimate on an individual takes about 10 s, with no operator postprocessing as in DXA required (or allowed).

As shown in Figure 2, the ultrasound signal propagates in three distinct pathways. One pathway consists of soft tissue only (a soft-tissue wave or "SW"); clinically, this corresponds to the space between the ulna and the radius at the 1/3 location. The time delay associated with this pathway is denoted by $\tau_{SW}$. Another pathway consists of propagation through soft tissue on both sides of the radius, propagation through two cortices on opposite sides of the radius and propagation through the marrow-filled medullary cavity as well (a direct wave or "DW"). The time delay associated with this pathway is denoted by $\tau_{DW}$. The final pathway consists of propagation through soft tissue on both sides of the radius and propagation through the radial cortex only (a circumferential wave or "CW"). The time delay associated with this pathway is denoted by $\tau_{CW}$. Thus, $NTD_{DW} = \tau_{SW} - \tau_{DW}$ and $NTD_{CW} = \tau_{SW} - \tau_{CW}$. Note that the physical separation of the radius and ulna at the 1/3 location in adults is nominally about 1 cm; therefore, the number of receiver elements associated with the soft-tissue only region (away from the bone edges) is about 10 and a SW time delay (*i.e.*, $\tau_{SW}$) can be estimated for each of these channels. A somewhat smaller number of channels (typically 5–10) is associated with propagation primarily though the radius and, from each of these channels, a pair of DW and CW time delays (*i.e.*, $\tau_{DW}$ and $\tau_{CW}$) can be estimated. The final estimates of the three time delays are obtained by averaging the set of delays associated with each channel. Note that the SW channels are identified by the large maximum absolute amplitudes associated with the signals that have propagated through soft-tissue only, whereas the "radius" channels are those whose amplitudes are smallest, adjacent to the soft-tissue only channels, and near the upper portion of the array (regardless of which arm is being measured; see Fig. 1).


Fig. 2. Schematic of radius bone showing three propagation pathways (see text).

Estimation of the time delays associated with the three pathways is described in (Luo et al., 2012; Luo and Kaufman 2011). Briefly, a set of signals associated with the soft tissue only path is first identified using the maximum absolute amplitude as a guide. (The peak absolute amplitudes of the SW signals are typically 30–40 dB larger than those associated with the CW and DW signals.) The mean time delay of this set of signals ("$\tau_{SW}$") is obtained by averaging the time delays, $\tau_{SWi}$, of each of the soft tissue signals in the identified set by a method of moments, computed over the first half-cycle of each signal:

$$\tau_{SWi} = \frac{\int_{t_{0i}}^{t_{1i}} t \cdot s_i^2(t)\, dt}{\int_{t_{0i}}^{t_{1i}} s_i^2(t)\, dt} \tag{1a}$$

and

$$\tau_{SW} = \sum_{i=1}^{N_{SW}} \tau_{SWi} \tag{1b}$$

In eqns (1a) and (1b), $s_i(t)$ is a soft tissue signal measured with an individual element (channel) of the array receiver transducer, $t_{0i}$ and $t_{1i}$ are the initial and final time points (linearly interpolated if necessary) of

the first half-cycle of the signal $s_i(t)$, and $N_{SW}$ is the number of receiver channels that are associated with propagation through the soft tissue pathway. As noted above, a typical soft-tissue time delay estimate includes about ten channels (dependent on forearm and bone sizes), and the use of the moment computation serves to reduce the influence of noise due to the integrations in (1a). The determinations of $\tau_{SW}$ and $\tau_{DW}$ are done entirely analogously to eqns (1a) and (1b), but utilizing a set of (about 5–10) channels associated with propagation through the radius.

It is hypothesized that each of the two NTD parameters is proportional to the amount of bone (*i.e.*, effectively proportional to BMD as would be measured by DXA) in their respective and distinctive pathways. This has been shown for $NTD_{DW}$ using computational, *in vitro* and clinical studies (Luo et al. 1999; Le Floch et al. 2008a, 2008b; Kaufman et al., 2007; Siffert and Kaufman 2007). Using geometrical arguments, $NTD_{CW}$ in combination with $NTD_{DW}$ has also been shown *in vitro* to provide an ultrasonic-based estimate, $BMD_{US}$, of radial DXA BMD at the 1/3 location, according to the following formula (Le Floch et al. 2008a):

$$BMD_{US} = a \cdot [NTD_{CW} \cdot NTD_{DW}]^{1/2} + b \qquad (2)$$

In eqn (2), $a$ and $b$ are regression parameters to be determined by the method of least squares.

For comparison purposes, an average ultrasound velocity (UV) associated with each subject was also evaluated. UV was defined as $d_{1/3}/\tau_{DW}$ where $d_{1/3}$ is the thickness of the forearm at the 1/3 location, (*i.e.*, the separation of the skin-contacting transducer pair).

*Clinical measurements*

Sixty adult subjects were recruited for this study under an IRB approved protocol and informed consent was received from each participant. Pregnancy was excluded in premenopausal women before DXA scans were performed. Each subject was measured three to five times at the 1/3 radius with the *UltraScan 650*. Standard off-the-shelf isopropyl alcohol (70%) was used as an ultrasound coupling agent; it was sprayed onto the subject's forearm and the transducers' active surfaces. The alcohol also served as an antiseptic and evaporated relatively quickly so that clean-up was minimal (as opposed to using standard coupling gel). The ultrasound device requires a minimum of three independent ultrasound measurements to be made on each person; if the range of both NTD parameters is sufficiently small (*viz.*, the range of both NTD parameters is within $\pm 0.05$ $\mu$s, which on average represents a precision of about 3%), the test ends. Otherwise, up to two more independent NTD measurements were made and the three closest together data sets were averaged and saved to a log file. For each subject radial bone density at the same 1/3 location was determined using DXA (QDR 4500; Hologic, Inc., Bedford, MA, USA). Finally, an ultrasound reproducibility study was carried out on three additional subjects each with 15 independent measurements and the percent coefficient of variation (%CV) was evaluated (Bonnick 2004).

## RESULTS

Table 1 lists the demographic and ethnic/racial data on the 60 subjects in this study. A set of received ultrasound waveforms associated with a typical subject is shown in Figure 3a. Two signals are displayed; one (solid line) is for a channel located largely behind the radius and the other (dotted line) is for a channel located behind a soft tissue only region. For purposes of the plot, the data from the soft tissue channel ("SW") has been divided by twenty so that the signals associated with propagation through the radius (*i.e.*, the CW and DW) may be clearly observed. Figure 3b displays the variation of the transit times associated with the three propagation pathways as a function of channel (receiver element) number for a typical study subject. As may be seen, each channel is associated generally with a distinct value of the associated time delay; as noted above (eqn [1b]), the actual estimate for a given time delay is computed as an arithmetic average of a small number of such individual channel delays that are centered around the regions directly behind the radius (indicated in Fig. 3b by the arrows for $\tau_{CW}$ and $\tau_{DW}$) and centered directly behind the region containing only soft tissue (indicated in Fig. 3b by the arrow for $\tau_{SW}$).

For these clinical data, plots showing the relationships of $BMD_{US}$ and UV to BMD, together with the respective linear regression curve fits, are shown in Figure 4a and b, respectively. The linear correlation between $BMD_{US}$ and BMD was $r = 0.93$ ($p < 0.001$);

Table 1. Demographic statistics for the clinical study group

| N = 60 (Number of subjects) | Mean (SD) | Min–Max |
|---|---|---|
| Age (y) | 47 (20) | 22–84 |
| Race | | |
| 62% White | | |
| 7% African American | | |
| 16% Hispanic | | |
| 15% Asian | | |
| Sex (68% female) | | |
| Height (cm) | 167 (11) | 150–198 |
| Weight (kg) | 73 (16) | 50–143 |
| 1/3 radius BMD (g/cm$^2$) | 0.69 (0.12) | 0.45–0.92 |

BMD = bone mineral density; SD = standard deviation; Min = minimum; Max = maximum.

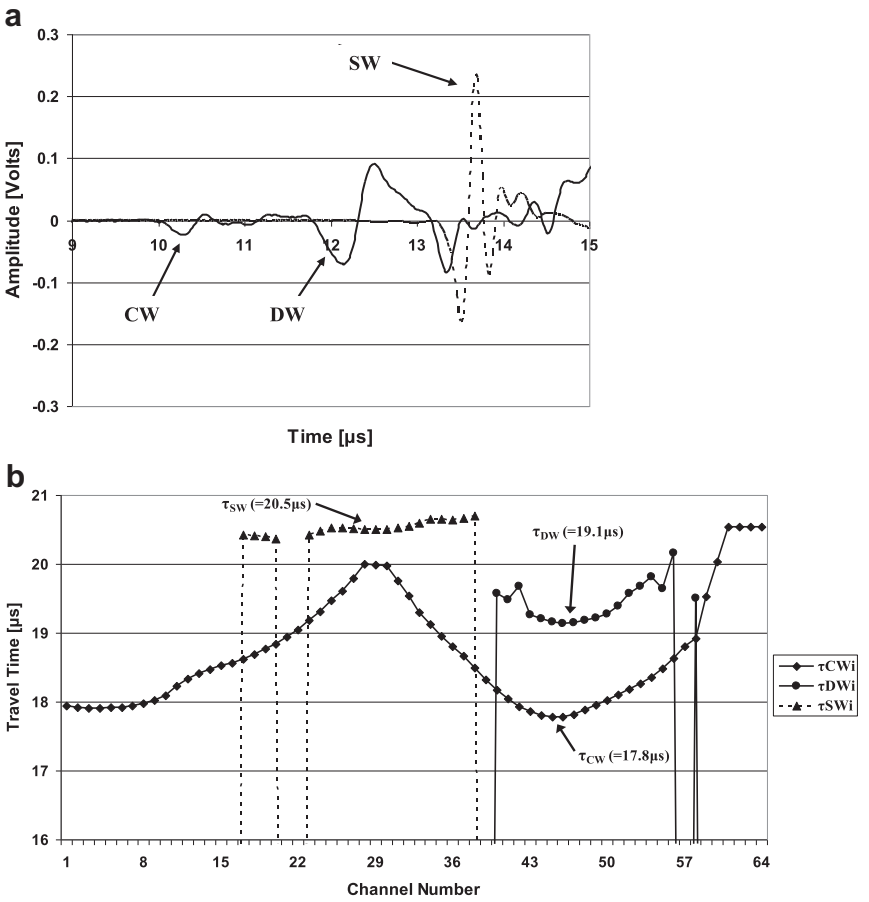


Fig. 3. (a) Plot of received waveforms for a typical subject. Two channels are shown; the solid line indicates a channel located largely behind the radius, whereas the dotted line indicates a channel within the soft tissue only region. For purposes of the plot, the data from the soft tissue channel ("SW") has been divided by 20 so that the signals associated with propagation through the radius (*i.e.*, the CW and DW) may be clearly observed. Thus, the actual voltage of the soft tissue only signal is approximately 4.6 volts. (b) Plot of the estimates of the three transit times $\tau_{DWi}$, $\tau_{CWi}$ and $\tau_{SWi}$ associated with the direct, circumferential and soft-tissue waves, respectively, as a function of channel (array element) number $i$, $i = 1,\ldots,64$. The actual estimates of the three transit times, $\tau_{DW}$, $\tau_{CW}$ and $\tau_{SW}$, are based on an average of three to five transit times near the minimum delays associated with each of the three modes, indicated by the arrows, respectively. See also eqn (1b) in the text.

the linear correlation between UV and BMD was r = 0.78 ($p < 0.01$). The linear univariate regression between BMD and $BMD_{US}$ produced a standard error of the prediction of 0.043 g/cm$^2$. The linear univariate regression between BMD and UV produced a standard error of the prediction of 0.077 g/cm$^2$. Finally, the percent coefficient of variation in the reproducibility study was found to be 2.1%.

## DISCUSSION AND CONCLUSION

The data presented demonstrate that the new device and its associated nonlinear function of two ultrasound NTD parameters, $NTD_{DW}$ and $NTD_{CW}$, is a very good proxy of BMD as measured by DXA at the 1/3 radius. In contrast, the data show that ultrasound velocity is much less correlated with BMD; this is a result of the variations between people in amount of overlying soft tissue thickness and size of the marrow-containing medullary cavity.

The results reported here are consistent with previously reported computational and *in vitro* studies. In particular, in a two-dimensional (2-D) computer simulation study on 20 human radii, $NTD_{DW}$ was shown to have a high correlation ($r = 0.99$, $p < 0.001$) with cortical thickness (Kaufman et al. 2008). The data from this simulation study were re-analyzed; the cross-sectional (bone-only) area of each radius was divided by the projected bone width to obtain the simulated BMD, $BMD_{SIM}$, in this case in units of millimeters of bone. (Note that the actual values of $BMD_{SIM}$ would normally need to be scaled by a factor related to the mineral density of bone but this is not done here as it is not relevant to this analysis; such a scale factor would only affect the associated regression coefficients.) The relationship between

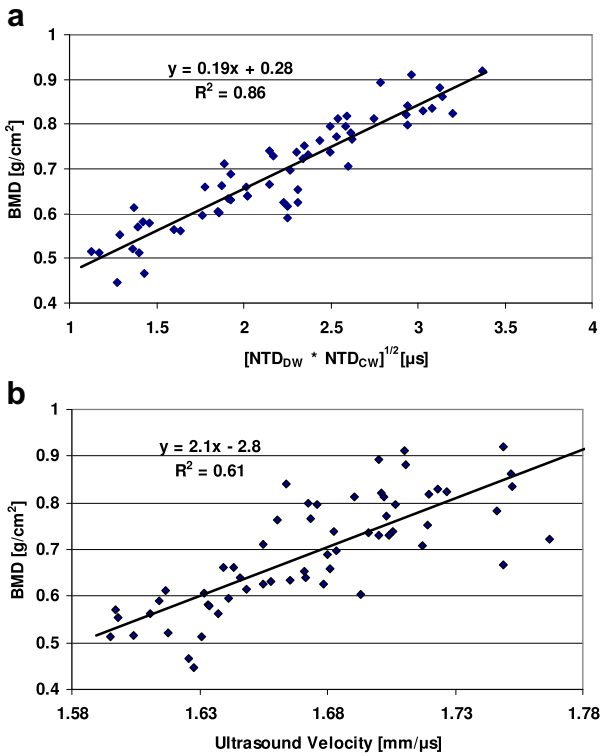


Fig. 4. (a) Plot of BMD vs. $[NTD_{CW} * NTD_{DW}]^{1/2}$ for the clinical study. (b) Plot of BMD vs. ultrasound velocity (UV) for the clinical study.

$BMD_{SIM}$ and the two NTDs is assumed to have the same form as in eqn (1). In this case $NTD_{CW}$ and $NTD_{DW}$ are replaced by $NTD_{CW\text{-}SIM}$ and $NTD_{DW\text{-}SIM}$, respectively, the latter pair being the simulated values of the two NTD parameters from Kaufman et al. (2008). Figure 5 displays the relationship for the simulated data. As may be seen, there is a high degree of correlation ($r = 0.96$, $p < 0.001$) between $BMD_{SIM}$ and the square root of the product of the two NTDs, similar to the clinical case. It should be noted that the simulation study demonstrated that the CW mode through the radii was similar to a circumferential guided wave through a cylinder that has been characterized analytically by Rose (1999). It should be noted that the nominal wavelength of the ultrasound propagating in the cortex is on the order of 1 mm (nominal center frequency of 3 MHz, nominal longitudinal velocity of 3000 m/s), which is in the range of cortical thicknesses typically observed (~0.5–2 mm). Thus, further studies that examine the dispersion curves of circumferential modes in irregular tubes should provide further insight into this key mode of propagation that is observed in transmission through the radius. An important consideration will be to develop dispersion curves for the case of tubes, which are loaded both inside and outside by soft tissue (*i.e.*, outside the radius by

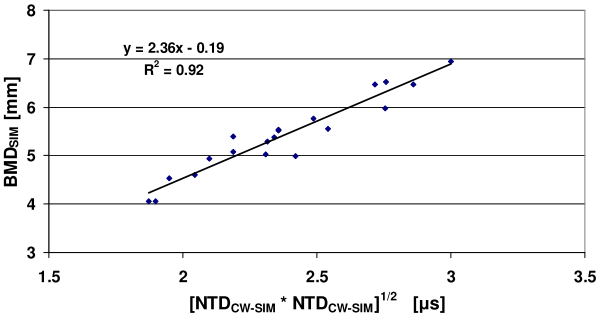


Fig. 5. Plot of $BMD_{SIM}$ vs. $[NTD_{CW\text{-}SIM} * NTD_{DW\text{-}SIM}]^{1/2}$ for a previous computational study.

muscle and fat and inside the radius by marrow/blood), to appropriately model the clinical reality.

The clinical results are also consistent with an *in vitro* study on the same set (less one) of 20 human radii (Le Floch et al. 2008a). The radii were scanned in a water tank with a laboratory prototype similar to the clinical *UltraScan 650*. The two NTD parameters were evaluated and shown to have a correlation ($r = 0.95$, $p < 0.001$) with the cross-sectional (bone) area (Le Floch et al. 2008a). To compare the *in vitro* results with the clinical data of this study, this data was also re-analyzed. The cross-sectional area was converted to an equivalent BMD (by dividing by the associated projected bone width), to obtain $BMD_{InVitro}$. (Note that $BMD_{InVitro}$ is equal to $BMD_{SIM}$ of the previous paragraph.) The relationship between $BMD_{InVitro}$ and the two NTDs is again assumed to have the same form as in eqn (1). In this case, $NTD_{CW}$ and $NTD_{DW}$ are replaced by $NTD_{CW\text{-}InVitro}$ and $NTD_{DW\text{-}InVitro}$, respectively, the latter pair being the *in vitro* values of the two NTD parameters from Le Floch et al. (2008a). Figure 6 displays the relationship for the *in vitro* data. As may be seen, there is a high degree of correlation ($r = 0.92$, $p < 0.001$) between $BMD_{InVitro}$ and the square root of the product of the two NTDs, again similar to the clinical case. The remarkably high degree of similarity in the computational, *in vitro* and clinical data lends strong support to the applicability of the NTD-based methods

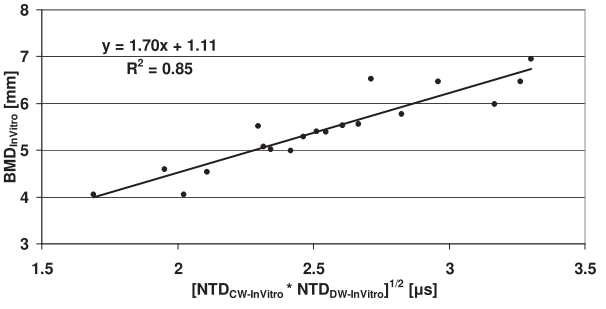


Fig. 6. Plot of $BMD_{InVitro}$ vs. $[NTD_{CW\text{-}InVitro} * NTD_{DW\text{-}InVitro}]^{1/2}$ for a previous *in vitro* study.

used for assessing BMD. Further research on extending ultrasound to assessing the ultra-distal radius is also underway (Le Floch et al. 2008b).

In summary a new device, the *UltraScan 650*, has been described that has the potential to enlarge the scope of ultrasound bone assessment in particular and of bone screening in general. The portability and simplicity in use of the radiation-free ultrasound scanner, combined with its high degree of accuracy and precision in estimating radial BMD, provides a basis by which to expand ultrasonic assessment to the primary care setting. This will in turn provide an opportunity to reduce the incidence of osteoporotic fractures through early and timely therapeutic interventions.

*Acknowledgments*—The kind support of the National Institute of Arthritis and Musculoskeletal and Skin Diseases (Grant Number AR45150) and the National Institute on Aging (Grant Number AG036879) of the National Institutes of Health, through the Small Business Innovative Research Program are gratefully acknowledged. The funders had no role in the design and conduct of the study; collection, management, analysis, and interpretation of the data; and preparation, review, or approval of the manuscript.

## REFERENCES

Anonymous. Osteoporosis prevention, diagnosis, and therapy. JAMA 2001;285:785–795.

Baim S, Leslie WD. Assessment of fracture risk. Curr Osteoporos Rep 2012;10:28–41.

Barkmann R, Kantorovich E, Singal C, Hans D, Genant HK, Heller M, Glüer CC. A new method for quantitative ultrasound measurements at multiple skeletal sites: First results of precision and fracture discrimination. J Clin Densitom 2000;3:1–7.

Blake GM, Fogelman I. Review–DXA scanning and its interpretation in osteoporosis. Hosp Med 2003;64:521–525.

Bonnick SL. Boned densitometry in clinical practice. Application and interpretation. 2nd edition. Totowa, NJ: Humana Press; 2004.

Hosokawa A. Effect of porosity distribution in the propagation direction on ultrasound waves through cancellous bone. IEEE Trans Ultrason Ferroelectr Freq Control 2010;57:1320–1328.

Johnell O, Kanis JA, Oden A, Johansson H, De Laet C, Delmas P, Eisman JA, Fujiwara S, Kroger H, Mellstrom D, Meunier PJ, Melton LJ III, O'Neill T, Pols H, Reeve J, Silman A, Tenenhouse A. Predictive value of BMD for hip and other fractures. J Bone Miner Res 2005;20:1185–1194.

Kanis J. Diagnosis of osteoporosis and assessment of fracture risk. Lancet 2002;359:1929–1936.

Kanis JA, Johansson H, Oden A, McCloskey EV. Assessment of fracture risk. Eur J Radiol 2009a;71:392–397.

Kanis JA, McCloskey EV, Johansson H, Oden A. Approaches to the targeting of treatment for osteoporosis. Nat Rev Rheumatol 2009b;5: 425–431.

Karjalainen JP, Töyräs J, Riekkinen O, Hakulinen M, Jurvelin JS. Ultrasound backscatter imaging provides frequency-dependent information on structure, composition and mechanical properties of human trabecular bone. Ultrasound Med Biol 2009;35:1376–1384.

Kaufman JJ, Einhorn TE. Review–Ultrasound assessment of bone. J Bone Miner Res 1993;8:517–525.

Kaufman JJ, Siffert RS. Noninvasive assessment of bone integrity. In: Cowin S, (ed). Bone mechanics handbook. Boca Raton, FL: CRC Press; 2001. p. 34.1–34.25.

Kaufman JJ, Luo GM, Siffert RS. A portable real-time bone densitometer. Ultrasound Med Biol 2007;3:1445–1452.

Kaufman JJ, Luo GM, Siffert RS. Ultrasound simulation in bone (invited paper). IEEE Trans Ultrason Ferroelectr Freq Control 2008;56: 1205–1218.

Kaufman JJ, Luo GM, Siffert RS. Effect of arm dominance on quantitative transmission ultrasound at the forearm. Thirty-first Annual Meeting of the American Society for Bone and Mineral Research. J Bone Miner Res 2009a;24(Supp S1):S319.

Kaufman JJ, Luo GM, Blazy B, Siffert RS. Quantitative ultrasound assessment of tubes and rods: Comparison of empirical and computational results. Proceedings of the 29th International Symposium on Acoustical Imaging. Acoustical Imaging. New York: Springer, 2009b;29:467–472.

Kilappa V, Moilanen P, Xu L, Nicholson PH, Timonen J, Cheng S. Low-frequency axial ultrasound velocity correlates with bone mineral density and cortical thickness in the radius and tibia in pre- and postmenopausal women. Osteoporos Int 2011;22:1103–1113.

King AB, Fiorentino DM. Medicare payment cuts for osteoporosis testing reduced use despite tests' benefit in reducing fractures. Health Aff (Millwood) 2011;30:2362–2370.

Krieg MA, Barkmann R, Gonnelli S, Stewart A, Bauer DC, Del Rio Barquero L, Kaufman JJ, Lorenc R, Miller PD, Olszynski WP, Poiana C, Schott AM, Lewiecki EM, Hans D. Quantitative Ultrasound in the Management of Osteoporosis: The 2007 ISCD Official Positions. J Clin Densitom 2008;11:163–187.

Langton CM, Palmer SB, Porter RW. The measurement of broadband ultrasonic attenuation in cancellous bone. Engl Med 1984;13:89–91.

Langton CM, Njeh CF. The measurement of broadband ultrasonic attenuation in cancellous bone—A review of the science and technology. IEEE Trans Ultrason Ferroelectr Freq Control 2008;55:1546–1554.

Langton CM, Langton DK. Comparison of bone mineral density and quantitative ultrasound of the calcaneus: Site matched correlation and discrimination of axial BMD status. Br J Radiol 2000;73:31–35.

Laugier P. Instrumentation for in vivo ultrasonic characterization of bone strength. IEEE Trans Ultrason Ferroelectr Freq Control 2008;55:1179–1196.

Laugier P, Haiat G, (eds). Bone quantitative ultrasound. Dordrecht, The Netherlands: Springer; 2011.

Lefebvre F, Deblock Y, Campistron P, Ahite D, Fabre JJ. Development of a new ultrasonic technique for bone and biomaterials in vitro characterization. J Biomed Mater Res 2002;63:441–446.

Leffall LD, Kripke ML. Reducing environmental cancer risk: What we can do now? President's Cancer Panel. Bethesda, MD: National Cancer Institute, National Institutes of Health, U.S. Department of Health And Human Services; 2010.

Le Floch V, Luo GM, Kaufman JJ, Siffert RS. Ultrasonic assessment of the radius in vitro. Ultrasound Med Biol 2008a;34:1972–1979.

Le Floch V, McMahon DJ, Luo GM, Cohen A, Kaufman JJ, Shane E, Siffert RS. Ultrasound simulation in the distal radius using clinical high-resolution peripheral-CT images. Ultrasound Med Biol 2008b;34:1317–1326.

Lewiecki EM, Laster AJ, Miller PD, Bilezikian JP. More bone density testing is needed, not less. J Bone Miner Res 2012;27:739–742.

Litniewski J, Cieslik L, Lewandowski M, Tymkiewicz R, Zienkiewicz B, Nowicki A. Ultrasonic scanner for *in vivo* measurement of cancellous bone properties from backscattered data. IEEE Trans Ultrason Ferroelectr Freq Control 2012;59:1470–1477.

Luo GM, Kaufman JJ, Chiabrera A, Bianco B, Kinney JH, Haupt D, Ryaby JT, Siffert RS. Computational methods for ultrasonic bone assessment. Ultrasound Med Biol 1999;25:823–830.

Luo GM, Kaufman JJ. Ultrasonic bone assessment apparatus and method, United States Patent No. 7,862,510, issued January 4, 2011.

Luo GM, Siffert RS, Johnson WA, Altman RL, Kaufman JJ. Ultrasonic bone assessment apparatus and method, United States Patent No. 8,202,219, Isued June 19, 2012.

Moilanen P. Ultrasonic guided waves in bone. IEEE Trans Ultrason Ferroelectr Freq Control 2008;55:1277–1286.

Melton LJ III. Epidemiology of fractures. In: Riggs BL, Melton LJ III, (eds). Osteoporosis: Etiology, diagnosis, and management. New York, NY: Raven Press; 1988. p. 133–154.

Miller CW. Survival and ambulation following hip fracture. J Bone Joint Surg 1978;60A:930–934.

Njeh CF, Fuerst T, Diessel E, Genant HK. Is quantitative ultrasound dependent on bone structure? A reflection. Osteoporos Int 2001; 12:1–15.

Ott SM, Kilcoyne RF, Chestnut CH III. Ability of four different techniques of measuring bone mass to diagnose vertebral fractures in postmenopausal women. J Bone Min Res 1987;2:201–210.

Padilla F, Jenson F, Bousson V, Peyrin F, Laugier P. Relationships of trabecular bone structure with quantitative ultrasound parameters: *In vitro* study on human proximal femur using transmission and backscatter measurements. Bone 2008;42:1193–1202.

Rose JL. Ultrasonic waves in solid media. Cambridge, UK: Cambridge University Press; 1999:154–157.

Siffert RS, Luo GM, Cowin SC, Kaufman JJ. Dynamical relationships of trabecular bone density, architecture and strength in a computational model of osteopenia. Bone 1996;18:197–206.

Siffert RS, Kaufman JJ. Ultrasonic bone assessment: "The Time Has Come." Bone 2007;40:5–8.

Souzanchi MF, Palacio-Mancheno PE, Borisov Y, Cardoso L, Cowin SC. Microarchitecture and bone quality in the human calcaneus; Local variations of fabric anisotropy. J Bone Miner Res 2012; Jul 13; http://dx.doi.org/10.1002/jbmr.1710 [Epub ahead of print].

Talmant M, Kolta S, Roux Ch, Haguenauer D, Vedel I, Cassou B, Bossy E, Laugier P. In vivo performance evaluation of bi-directional ultrasonic axial transmission for cortical bone assessment. Ultrasound Med Biol 2009;35:912–919.

Turner CH. Bone strength: Current concepts. Ann N Y Acad Sc 2006; 1068:429–446.

Wear KA. Measurements of phase velocity and group velocity in human calcaneus. Ultrasound Med Biol 2000;26:641–646.

Wear KA. Ultrasonic scattering from cancellous bone: A review. IEEE Trans Ultrason Ferroelectr Freq Control 2008;55:1432–1441.

Zhang J, Delzell E, Zhao H, Laster AJ, Saag KG, Kilgore ML, Morrisey MA, Wright NC, Yun H, Curtis JR. Central DXA utilization shifts from office-based to hospital-based settings among Medicare beneficiaries in the wake of reimbursement changes. J Bone Miner Res 2012;27:858–864.